International Journal of Disaster Risk Reduction 131 (2025) 105919

Contents lists available at ScienceDirect

International Journal of Disaster Risk Reduction

journal homepage: www.elsevier.com/locate/ijdrr

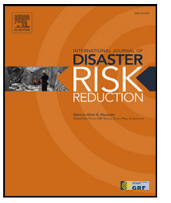

Use of mobile phone data to measure behavioral response to SMS evacuation alerts☆

Erick Elejalde [a,*], Timur Naushirvanov [b], Kyriaki Kalimeri [c], Elisa Omodei [b], Márton Karsai [b,d], Loreto Bravo [e], Leo Ferres [c,e,**]

[a] L3S Research Center, Leibniz University Hannover, Hannover, Germany
[b] Department of Network and Data Science, Central European University, Vienna, Austria
[c] ISI Foundation, Turin, Italy
[d] National Laboratory for Health Security, HUN-REN Rényi Institute of Mathematics, Budapest, Hungary
[e] IDS UDD, Santiago, Chile

ARTICLE INFO

Keywords:
Alerts
Human mobility
Crisis response
Mobile phone data (XDRs)
Population displacement

ABSTRACT

This study examines behavioral responses after mobile phone evacuation alerts during the February 2024 wildfires in Valparaíso, Chile. Using anonymized mobile network data from 580,000 devices, we analyze population movement following emergency SMS notifications. Results reveal three key patterns: (1) initial alerts trigger immediate evacuation responses with connectivity dropping by 80% within 1.5 h, while subsequent messages show diminishing effects; (2) substantial evacuation also occurs in non-warned areas, indicating potential transportation congestion; (3) socioeconomic disparities exist in evacuation timing, with high-income areas evacuating faster and showing less differentiation between warned and non-warned locations. Statistical modeling demonstrates socioeconomic variations in both evacuation decision rates and recovery patterns. These findings inform emergency communication strategies for climate-driven disasters, highlighting the need for targeted alerts, socioeconomically calibrated messaging, and staged evacuation procedures to enhance public safety during crises.

1. Introduction

Wildfires represent one of the most pressing environmental and societal challenges of the 21st century, driven by a combination of climate change, land-use policies, and human activities [1,2]. The impact of extensive wildfires like the ones experienced in California [3] or the Amazon rain-forest [4] goes beyond the local scale, affecting climate patterns, human health, and the economy [5–7]. While the evacuation procedures of wildfires are well-documented [8], the role of near-real-time communication technologies in shaping human responses to these crises remains less understood. Rapid and structured evacuation is critical to minimize loss of life during wildfires, yet human decision-making in such high-stress situations is influenced by multiple factors, including message timing, perceived risk, and socioeconomic status.

☆ LF thanks Telefónica Chile for funding and support. This research was supported by FONDECYT Grant No. 1221315 to LF. LF, KK acknowledge support from the Lagrange Project of ISI Foundation funded by CRT Foundation, Italy. MK acknowledges funding from the National Laboratory for Health Security (RRF-2.3.1-21-2022-00006), the ANR project DATAREDUX (ANR-19-CE46-0008); the SoBigData++ H2020-871042; the MOMA WWTF; and the COLINE DUT-FFG projects.

* Correspondence to: Applestraße 4, 30167, Hannover, Germany.
** Correspondence to: Av. Plaza 680, Las Condes, Santiago, Chile.
E-mail addresses: elejalde@l3s.uni-hannover.de (E. Elejalde), lferres@udd.cl (L. Ferres).

https://doi.org/10.1016/j.ijdrr.2025.105919
Received 2 May 2025; Received in revised form 5 October 2025; Accepted 17 November 2025
Available online 19 November 2025

The widespread penetration of mobile technology has transformed emergency alert systems into essential tools for crisis management, enabling the rapid dissemination of evacuation directives, curfews, and updates on available assistance [9]. As of 2024, there are 112 mobile-cellular subscriptions per 100 inhabitants [10] worldwide, and Chile is in line with this trend, reporting 133 phones per 100 inhabitants as of June 2024 [11]. This ubiquity has positioned Short Message Service (SMS) notifications as a viable and widely adopted method for mass communication during crises. A key advantage of SMS-based alerts is their ability to function on basic mobile phones without requiring Internet connectivity. Moreover, SMS is particularly effective in reaching diverse populations, including those in remote or low-resource settings, ensuring timely access to critical information. Building on the effectiveness of SMS, the Wireless Emergency Alerts (WEA) system was developed to send geo-targeted emergency messages to mobile devices by authorized public safety officials [12]. WEAs, operating via cell broadcasting, deliver warnings within seconds, without the need for a subscription or internet connection [13]. By integrating SMS capabilities with advanced alerting systems like WEA, governments have enhanced emergency communications, ensuring rapid, reliable, and inclusive public warnings in times of crisis [14]. These systems have demonstrated critical in saving lives and managing emergencies effectively. One of the earliest recorded cases of SMS for emergency alerts dates back to 19 September 2007, when the Disaster Management Center of Sri Lanka sent a 20-word text alert following a magnitude 7.9 earthquake off the southern coast of Sumatra [15]. During the 2010 Haiti earthquake, humanitarian organizations used SMS to coordinate rescue efforts and provide vital information to affected people [16]. During the outbreaks of Ebola in Liberia and Sierra Leone, SMS was used to spread public health messages and combat misinformation, significantly aiding disease control efforts [17–19] and even controlling the spread of disease-associated rumors [20]. In Japan, the J-Alert National Early Warning System serves as the country's primary platform for rapidly disseminating critical information to the public [21].

Despite the demonstrated utility of SMS and alert systems in crisis management [22], their effectiveness in prompting protective action remains an open question. To date, the main evaluation of the messaging effectiveness relied on surveys [23] and agent-based models [24]. Such approaches offer valuable insights, but are still prone to self-reporting biases regarding actual human behavior during disasters, which is shown to be influenced by the timing, content, and perceived credibility of risk communication [25–27].

While access to high-resolution mobility data has improved in recent years, what remains underexplored is the joint analysis of these data with the operational logic of public warning systems, enabling these data to act as a proxy for near-real-time evacuation patterns.The main reason stems primarily from the lack of accessible, high-resolution data that can act as a proxy to assess near-real-time evacuation patterns. Hence, gaps persist in understanding how individuals interpret and respond to emergency messages in real-world wildfire events. Do initial alerts trigger immediate evacuation, or does repeated exposure to messages induce alert fatigue, leading to reduced responsiveness? Are individuals from different socioeconomic backgrounds equally likely to heed evacuation warnings, or do structural inequalities create disparities in mobility and safety? Here, we aim at addressing these questions by coupling high-resolution mobility signals with emergency alerts, offering a powerful lens on evacuation dynamics at operational timescales.

The physical devastation of the wildfires that erupted at Valparaíso in Chile on February 2nd, 2024, was the most severe in the country over the last three decades. It caused 137 deaths, made 1600 others homeless, and directly affected more than 16,000 people [4], with the Chilean Government, as a consequence, declaring a State of Emergency and Catastrophe. Chile has also implemented a similar SMS-based warning system, the *Sistema de Alerta de Emergencia* (SAE), following the 27 February 2010 earthquake, to enhance public warnings for natural disasters. Since March 2017, all mobile phones sold in Chile have supported SAE at no additional cost to users, ensuring accessibility regardless of phone balance. From 2019 onward, mobile devices in Chile have come with SAE pre-configured by default [28]. This study leverages anonymized mobile network data to examine population-wide behavioral responses following evacuation alerts. More specifically, our study addresses three key research questions regarding behavioral responses, effectiveness, and unintended consequences of emergency messaging: First, *how does the timing and sequence of emergency alerts influence evacuation behavior?* Initial alerts may prompt a stronger response due to their urgency and element of surprise, while follow-up messages may be perceived as repetitive or less critical, potentially leading to alert fatigue and diminished compliance. Understanding this dynamic is crucial for optimizing the timing, frequency, and content of alerts to maintain public engagement without causing desensitization [25,29]. Second, *to what extent do socioeconomic factors shape evacuation patterns?* Socioeconomic status influences access to evacuation resources, comprehension of emergency messages, and trust in authorities [8,30]. Higher socioeconomic groups (SEG) of individuals may have better access to transportation and multiple information sources, enabling quicker and more independent responses. In contrast, lower SEG may face barriers such as limited mobility and historical mistrust of government-issued alerts, which could hinder effective evacuation. Addressing these disparities is essential for ensuring equitable crisis response strategies [31]. Third, *what are the unintended consequences of non-targeted alerts on population movement?* Broadly disseminated emergency messages can trigger unnecessary evacuation in areas not directly threatened by wildfires, potentially straining transportation infrastructure and emergency resources, diverting them from areas in need [31], while they can also have political implications [32].

Our study contributes to the growing literature on human adaptation to environmental hazards by integrating high-resolution behavioral data with policy-relevant questions. As climate change exacerbates wildfire risk globally, optimizing emergency communication strategies will be critical to enhancing public safety and resilience.

2. Background literature

A systematic review of evacuation from natural disasters [8] shows that compliance is shaped by risk perception, trust, and situational constraints. Communication science studies emphasized message credibility and clarity as determinants of protective action [25,33]. More recent studies have refined this perspective by investigating message characteristics such as length [23],

content [27], and sequencing. Yet repeated exposure can produce alert fatigue, where responsiveness diminishes over time, as noted in wildfire contexts [3,34]. These findings highlight the continuing debate over how to balance urgency with sustained compliance.

A substantial body of work has demonstrated that evacuation decisions are stratified across social and economic lines. Dash and Gladwin [29] identified household-level differences in decision-making, while Yabe et al. [35] quantified how income disparities affect evacuation, return, and recovery patterns. Trust in authorities has also been shown to shape compliance, particularly among vulnerable groups [30]. Recent advances using high-resolution mobility data have reinforced these insights: Deng et al. [36] revealed pronounced race- and wealth-based disparities in evacuation capacities across U.S. disasters. Together, these works underscore that structural inequalities are central to understanding evacuation dynamics.

Beyond surveys and interviews, the increasing availability of digital traces offers opportunities to study evacuation at scale. Mobile phone data have been applied to migration and displacement [6], social disparities in mobility [37,38], and post-disaster recovery [39]. Reviews highlight the potential of such data to overcome self-report bias and provide near real-time monitoring [22,31]. Recent applications illustrate these capabilities: Li et al. [40] used human mobility data to detect evacuation patterns during Hurricane Ian, demonstrating the operational value of geospatial analyses. However, most existing work has examined either inequality or evacuation detection in isolation, leaving underexplored the interaction between formal alerting systems and observed mobility patterns.

While there is robust evidence on warning design, behavioral response, and inequality, most of the studies remain confined to ex-post surveys, qualitative syntheses, or experimental settings. Few studies provide near-real-time, quantitative evidence of population responses to operational alert systems during fast-evolving disasters. We contribute to the existing gaps literature in the following ways. First, the immediate effectiveness of alerts and the risk of alert fatigue remain poorly quantified in real-world contexts. Second, socioeconomic disparities in evacuation, though widely recognized, are rarely measured dynamically with behavioral data. Third, while recent work such as Deng et al. [36] and Li et al. [40] demonstrates the power of high-resolution mobility data, these studies do not examine how populations react to official alerts in operational timescales.

By addressing these gaps, the present study contributes novel empirical evidence on the temporal, socioeconomic, and spatial dimensions of evacuation during the 2024 Valparaíso wildfires, uniquely combining operational alert data with fine-grained mobility records in a large-scale real-world setting. In relation to prior literature, this study advances the scientific understanding of evacuation and alert systems in three ways: (i) **Linking alert dissemination and mobility.** Our work directly connects operational SMS alerting with observed evacuation patterns, bridging a gap between communication studies and mobility analysis. (ii) **Quantifying inequalities with behavioral evidence.** We extend findings on socioeconomic disparities [35,36] by capturing stratified evacuation responses with high-resolution mobile network data. (iii) **Extending mobility-based disaster research to wildfires.** While recent advances have focused on hurricanes and floods [31,40], this study provides one of the first large-scale analyses of wildfire evacuations using digital traces, highlighting both responsiveness and alert fatigue. Together, these contributions offer new empirical insights that strengthen theoretical models of evacuation, advance understanding of alert effectiveness, and support the design of more equitable disaster risk reduction policies.

3. Results

On February 2, 2024, at 16:45, the first official evacuation alert was issued to towers in the Valparaíso region (Table A.2 shows the analyzed messages). The Valparaíso region (Fig. 1A) lies along the central coast of Chile between approximately 32° 02′ and 33° 57′ South latitude and 70° 00′ and 71° 43′ West longitude. The region spans an area of 16,396 square kilometers and is characterized by diverse topography, including coastal plains, the Coastal Mountain Range, and portions of the Andes Mountains. The region has a Mediterranean climate, characterized by dry summers that make it prone to wildfires and mild, wet winters. It houses a population of roughly 1.8 million inhabitants, with the majority concentrated in the Greater Valparaíso metropolitan area. The region's capital, Valparaíso city, is a UNESCO World Heritage site located approximately 120 kilometers northwest of Santiago, Chile's capital.

3.1. Phases of evacuation response in connectivity patterns

We analyzed anonymized phone network data aggregated over 15-minute intervals; Fig. 1B depicts the near-real-time device activity in reference to the baseline period (see Section 5). We notice that prior to the first evacuation alert, the connectivity patterns–that is, the number of unique active mobile phones in the different towers–aligned closely with baseline days measurements, with the connectivity to follow the expected circadian pattern with more connections and variability during day hours [41]. However, an anomaly is observed right before and after the first alert, indicating a deviation from the normal connectivity patterns. This response evolves in three distinct phases. The initial phase, preceding the evacuation alert, exhibits an increase in activity that lasted until shortly after the first alert. This phase shows several spikes to a maximum average of approximately 658 (95% CI 592, 723) connections for a 50% increase on the baseline average. This surge suggests heightened mobile phone usage outside WiFi coverage, possibly driven by information-seeking behavior and coordination efforts. In this sense, the SMS alert appears to have functioned as an official confirmation of an already perceived risk rather than the sole trigger of evacuation behavior. A second phase followed with a large drop, sinking to 132 connections on average (95% CI 97, 167), indicating rapid population displacement from the area. Despite multiple subsequent alerts (see Fig. 4), connectivity levels gradually stabilized to pre-alert values over an 8-hour period, returning to a circadian pattern around 00:00-01:00 on February 3 and starting a third phase of recovery. The second day (recovery phase) exhibited sustained elevated activity 40%–20% above typical patterns, with altered temporal signatures persisting throughout the observation period. This suggests enduring modifications to local connectivity patterns following the emergency event. Notably,

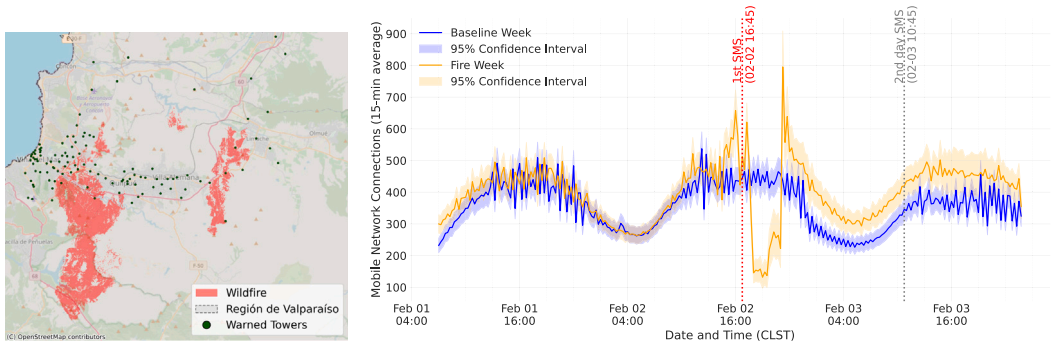

(a) (b)

Fig. 1. Mobile phone tower connectivity patterns and location during a wildfire evacuation event. A. General geographic area of the fires (in red) along with the warned towers (green dots). **B**. Time series comparing average mobile tower connections during baseline days (blue) and fire week (orange) in February 2024, with 95% confidence intervals (shaded areas). Vertical lines indicate critical emergency communication times: first evacuation alert (red, February 2, 16:45) and first alert of day two (gray, February 3, 10:45). The data reveals distinct behavioral patterns following the initial evacuation alert, including an immediate spike in connectivity followed by a rapid decrease, suggesting population displacement.

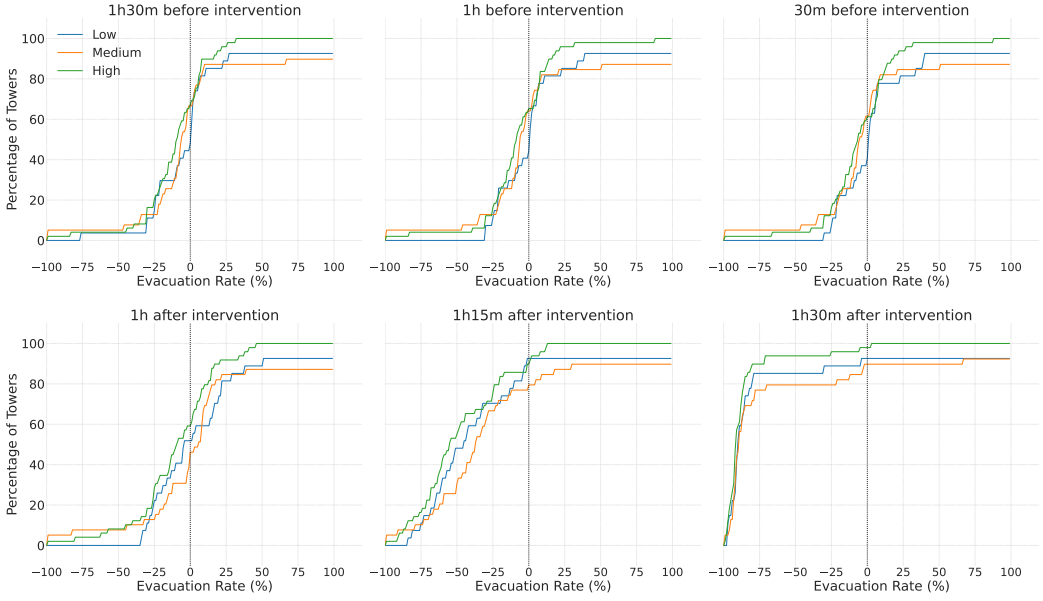

Fig. 2. Snapshots of the Cumulative distribution functions (CDFs) of tower-level evacuation rates with respect to the baseline behavior, stratified by socioeconomic status. The figure presents six time-sliced CDFs capturing activity patterns before and after the intervention across low (blue), medium (orange), and high (green) socioeconomic areas. The top row of the panel shows the pre-intervention behavior at 90 min, 1 h, and 30 min, respectively, while the second row in the panel indicates the post-intervention behavior displaying changes at 1 h, 75 min, and 90 min after the intervention. The x-axis represents the percentage of the evacuation rate, where the "0" rate indicates a consistent behavior with the baseline days. The negative rates indicate an evacuation behavior with respect to the baseline, while the positive rates represent more connections with respect to the baseline. The y-axis expresses the cumulative percentage of towers exhibiting evacuation rates lower or equal to the corresponding evacuation rate in time (x-axis).

the first alert of the second day showed no visible effect on connectivity patterns, unlike the response afterto the initial evacuation message, highlighting the diminishing effectiveness of repeated alerts and potential alert fatigue.

Diving into the socioeconomic disparities, we stratify by socioeconomic groups (see Supplementary Fig. B.7), and differences become apparent, particularly during the recovery phase. High-income areas show less variability in the average number of connections and return to baseline ranges faster. This suggests that populations in wealthier regions experience fewer barriers to evacuation and recovery, such as alternative housing options.

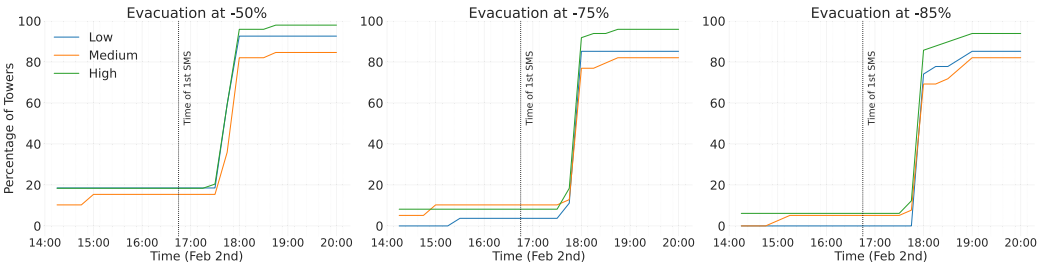

Fig. 3. Cumulative distribution functions of tower evacuations over time. The *y*-axis indicates the percentage of towers that reached the specified evacuation rates (50%, 75%, and 85%) at a specific time (x-axis). We stratified by socioeconomic groups: low (blue line), medium (orange line), and high (green line). The dashed line marks the time at which the first evacuation alert was sent.

3.2. Evacuation temporal dynamics and socioeconomic disparities

The cumulative distribution functions of tower-level evacuation rates relative to baseline behavior (i.e., percentage of connected devices compared to baseline days) (see Fig. 2) further reveal distinct temporal patterns in device activity across the three socioeconomic groups (low, medium, and high) before and after the alert intervention. In the pre-intervention period (1 h 30 min to 30 min to intervention), activity patterns remained broadly consistent with baseline behavior, as indicated by the clustering of CDFs around the zero point of the evacuation rate. The figure shows that most towers stay within ±25% of the baseline during this time. However, a marked divergence emerged post-intervention, particularly at 1 h and 15 min since the alert. At this time point, approximately 60% of towers in high socioeconomic areas showed a 50% evacuation rate, compared to roughly 50% in low and less than 30% in medium socioeconomic areas. The separation between socioeconomic groups became most pronounced at 1 h 30 min post-intervention, where high socioeconomic areas exhibited the strongest evacuation response, with nearly 90% of towers showing at least 75% evacuation. In contrast, in low and medium areas, only 85% and 77% of the towers reach the same evacuation rate, respectively. The observed response across socioeconomic categories suggests that the alert intervention triggered an unequal evacuation behavior, with populations in higher socioeconomic areas demonstrating substantially greater activity changes in warned towers. Notably, the steepness of the CDF curves in the post-intervention period, particularly between 1 h 15 min and 1 h 30 min, indicates a relatively uniform response within each socioeconomic group, suggesting coordinated population movement patterns that reflect underlying social and economic disparities in evacuation capacity.

To zoom in on the evacuation temporal patterns and the delay followingin response to the first system-wide evacuation alert, we also plot the cumulative distribution over time for the percentage of towers at different evacuation rates (50%, 75%, and 85%) (Fig. 3), where 100% is complete evacuation, meaning towers had no connections. Prior to the alert (marked by the vertical dashed line at 02-02 16:45), all socioeconomic groups showed minimal evacuation activity between 14:00 and 16:45. Following the evacuation alert, there was a dramatic and nearly simultaneous response across all groups. Among all evacuation rates, high socioeconomic areas demonstrated the most vigorous response, with over 95% of their towers showing at least 50% evacuation within 1 h and 15 min of the alert (by 02-02 18:00), compared to 92% for low and 82% for medium socioeconomic areas. The socioeconomic gradient became more pronounced at higher evacuation rates. At the 75% evacuation level, while high socioeconomic areas maintained nearly 92% compliance by 18:00, medium socioeconomic areas showed a reduced response of approximately 77% of towers, and low socioeconomic areas dropped to about 85%. The disparity is most stark at the 85% evacuation rate, where by 18:00, about 86% of towers in high socioeconomic areas, 69% in medium areas, and 74% in low socioeconomic areas achieved this evacuation level. These patterns suggest that while the alert triggered an immediate response within the first 1 h and 15 min across all socioeconomic groups, the capacity to achieve higher levels of evacuation was strongly influenced by socioeconomic status.

The temporal CDF plots show that low SEG towers were slower to start with the evacuation process at higher rates (e.g., reaching evacuation rates above 75%) than medium SEG towers. However, after 1 h and 15 min, they reacted, and by 1 h and 30 min after the first evacuation alert, approximately 85% of the low SEG towers had reached a 75% evacuation rate, overcoming the 77% of medium SEG towers at the same evacuation rate. This indicates a higher impact of the event on the lower SEG while maintaining a longer reaction time. The high SEG towers are the fastest in reaction time and most compliant with evacuation. The figures show that almost 95% of high SEG towers reached over 75% evacuation rate within 1 h and 30 min after the first system-wide alert. This reveals their higher reaction capacity to emergency events. However, when considering the behavior of non-affected towers, the pattern observed for high SEG areas may also point to an overreaction to the warning alerts.

3.3. Measuring population displacement and socioeconomic disparities

To facilitate a standardized comparison across heterogeneous spatial units, we introduce the Relative Evacuation Index (REX), a normalized metric for quantifying population displacement, defined as:

$$\mathrm{REX} = \frac{n_t - n_b}{n_t + n_b}$$

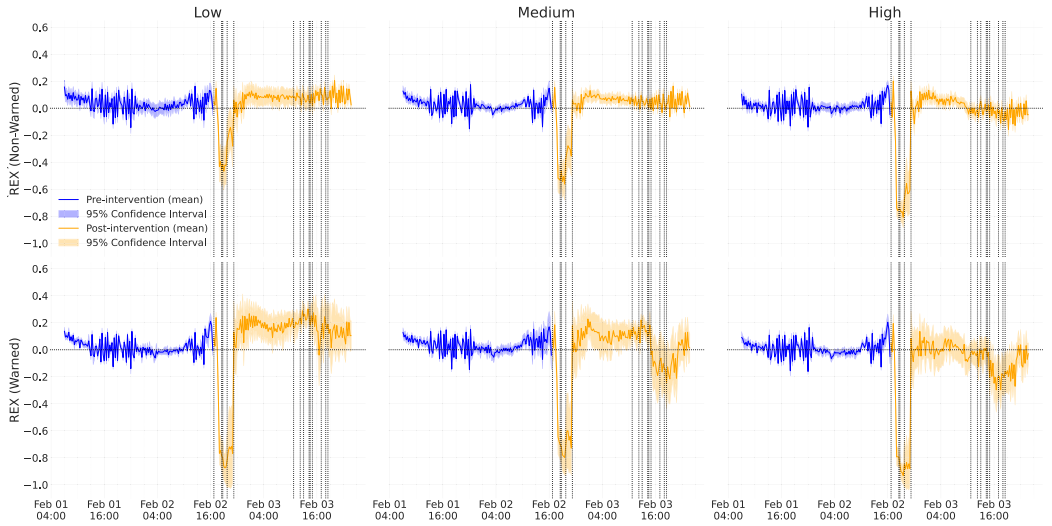

Fig. 4. Relative Evacuation Index for non-warned (upper panel) and warned towers (lower panel), across SEGs before and after the first evacuation alert. The blue lines represent pre-warning periods, while the orange lines indicate post-warning periods. Vertical dashed lines correspond to the times when evacuation alerts were sent. Panels are divided by SEG (low, medium, high) and whether towers were warned or non-warned. The shaded regions indicate 95% confidence intervals. The figure illustrates behavioral differences in evacuation responses and recovery patterns across SEGs and between warned and non-warned areas.

where n_t represents the number of unique mobile devices detected in a given spatiotemporal unit at time t, and n_b denotes the device count for the corresponding spatiotemporal unit in the baseline days. This formulation maps the relative population change onto the interval [−1, 1]. REX exhibits several desirable methodological advantages: it maintains symmetry around zero, ensures scale invariance across different population densities, and exhibits stability compared to conventional percentage-based measures, particularly when baseline populations are small. The resulting index provides an intuitive interpretation where negative values indicate net population egress, positive values suggest population ingress, and the magnitude reflects the relative strength of displacement. Supplementary Figs. C.8 and C.9 show the cumulative distribution functions using REX instead of the evacuation rate (cf. Figs. 2 and 3 above).

We find that both warned and non-warned towers reacted strongly to the evacuation alert (see Fig. 4). In non-warned towers, the REX reached −0.47 (95% CI, −0.60, −0.33) for the low SEG, −0.56 (95% CI, −0.68, −0.44) for the medium SEG, and −0.81 (95% CI, −0.88, −0.73) for the high SEG. This indicates that many people chose to leave the area regardless of whether they received the message addressing them directly or not. These findings have important policy implications, as individuals not directly affected by the warning may still attempt to evacuate, potentially congesting main roads and impacting those required to evacuate. While non-warned areas show evacuation behavior in general, the response is stronger among towers in the high SEG compared to those in the low and medium SEGs. Specifically, while REXthe evacuation rate approximately doubles for low −0.87 (95% CI, −0.98, −0.77) and medium −0.80 (95% CI, −0.93, −0.66) SEGs when their communities are directly addressed (warned towers), the difference between warned and non-warned towers in the high SEG is only around 15%, increasing from −0.81 in non-warned towers to −0.93 (95% CI, −1.00, −0.86) in warned towers. As observed before, SEG differences do not significantly affect the time required for these areas to reach the lower REX (all between 18:30 and 19:30). However, they do influence the intensity of the effect and behavior during the recovery phase between the last message on February 2 and the end of the observed period.

High SEG evacuees return to normal levels faster than those in the low and medium SEGs, practically skipping the recovery phase observed in other groups. Low SEG evacuees maintain a stable 20% increase over the baseline, while medium SEG evacuees stabilize at around 10%. A notable effect is observed succeedingin response to the second batch of evacuation messages on February 3: high SEG shows a stronger reaction again, reaching a mean REX of −0.25. The medium SEG reaches −0.20, though this is not a statistically significant deviation from the baseline at the 95% CI, while the low SEG does not show a noticeable change and remains above the baseline. As observed before, the REX measurements show that warning messages sent during the second day do not prompt the same reaction seen for the initial SMSs on the previous day, even for communities that were first notified on February 3rd (see Figs. D.10 and D.11). Note that, unlike on the first day, the differentiated reaction during the second day for the high SEG might be explained, at least in part, by the distribution of the affected areas, where more than half of the notified towers belong to the high SEG. To isolate the intervention's true impact across SEGs, we used non-affected towers as a baseline control. This approach allowed us to distinguish intervention-specific responses from general panic-motivated behavior. Notably, while affected areas showed distinct response patterns, non-affected towers quickly returned to pre-intervention activity levels without a recovery phase. The difference in REX between affected and non-affected towers reveals clear socioeconomic patterns (Fig. 5). During the pre-intervention period, no SEG showed significant behavioral deviations from the previous week. However, following the first

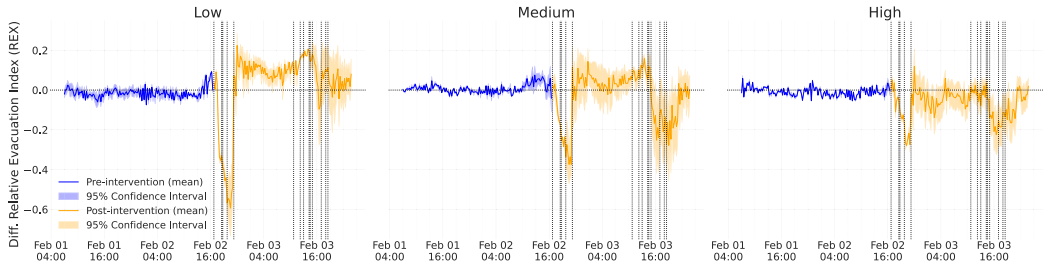

Fig. 5. Differential REX over time stratified by three socio-economic groups (Low (left), Medium (center), and High (right)) from February 1-3, 2024. We depict the pre-intervention (blue) and post-intervention (orange) time series, with their respective 95% confidence intervals, and measurements taken every 15 min. The dashed lines are all the evacuation alerts sent.

Table 1
Controlled Interrupted Time Series (CITS) Model for different socioeconomic groups (SEG).

	Socio-Economic Groups (Feb 2nd)			Socio-Economic Groups (Feb 3rd)		
	Low	Medium	High	Low	Medium	High
N	8143	10 189	15 804	8283	10 018	15 588
R^2	0.289	0.329	0.427	0.025	0.026	0.032
Intercept	−0.051***(−0.081–0.022)	−0.045***(−0.067–0.023)	−0.053***(−0.075–0.032)	0.141*(0.012-0.271)	0.256***(0.179-0.333)	0.487***(0.399-0.576)
T	0.001***(0.0-0.001)	0.001***(0.0-0.001)	0.001***(0.0-0.001)	0.0(−0.001-0.0)	−0.001***(−0.001–0.001)	−0.002***(−0.003–0.002)
I_0	−0.393***(−0.433–0.353)	−0.463***(−0.498–0.428)	−0.675***(−0.7–0.651)	−0.002(−0.028-0.024)	−0.003(−0.018-0.011)	0.005(−0.014-0.023)
T_{I_0}	0.026***(0.023-0.029)	0.031***(0.029-0.034)	0.045***(0.044-0.047)	0.001(−0.0-0.002)	0.001***(0.001-0.002)	0.002***(0.001-0.002)
G	−0.065**(−0.107–0.022)	−0.054*(−0.099–0.01)	−0.042*(−0.077–0.007)	0.128(−0.124-0.381)	0.0(−0.226-0.226)	−0.228(−0.467-0.01)
GT	0.0*(0.0-0.001)	0.001*(0.0-0.001)	0.0(0.0-0.001)	0.0(−0.002-0.001)	0.0(−0.001-0.001)	0.001(0.0-0.002)
GI_0	−0.36***(−0.421–0.3)	−0.242***(−0.302–0.182)	−0.114***(−0.156–0.073)	0.054*(0.004-0.104)	−0.046*(−0.091–0.002)	−0.073**(−0.121–0.025)
GT_{I_0}	0.03***(0.025-0.036)	0.015**(0.01-0.02)	0.005*(0.001-0.009)	−0.003***(−0.005–0.001)	−0.004***(−0.005–0.002)	−0.001(−0.003-0.001)

Note: $^{*}p < 0.05$; $^{**}p < 0.01$; $^{***}p < 0.001$

evacuation alert, the magnitude of the adjusted REX decline correlated directly with the tower locations' socioeconomic status, with the strongest effects observed in low-income areas. In contrast, high-SEG communities showed minimal changes in the adjusted REX, suggesting these populations would likely have evacuated regardless of whether they were in affected areas (see also Table 1).

Note that REX measurements during the recovery phase capture net connectivity patterns but cannot distinguish between returning residents and other populations entering the area. The return to baseline REX values could reflect original residents returning, emergency responders arriving, journalists covering the aftermath, or a combination of these groups. While the scale of resident populations relative to temporary responders suggests that residents likely dominate the observed patterns, and the gradual recovery over 8 h aligns more with resident return than emergency deployment, we cannot definitively determine population composition from connectivity data alone. This limitation should be considered when interpreting the recovery patterns and socioeconomic differences we observe in the post-evacuation period.

3.4. Impact of warning alerts on evacuation and return dynamics

We used a controlled interrupted time series (CITS) analysis to evaluate the causal effect of the warning alert intervention during the initial 24-hour period (see Section 5 below). Analysis of the pre-intervention temporal trends revealed no significant association between the REX and time for either the treatment or control groups ($\beta_1 \approx 0$ and $\beta_5 \approx 0$, respectively)(see Table 1). The statistical models demonstrated that SEGs maintained consistent connectivity patterns during the pre-intervention period relative to the baseline days, indicating stability in connectivity behavior prior to the intervention. Also, analysis of baseline differentials (G coefficient) revealed minimal variations across SEGs, with relatively small magnitude differences ($\delta < 0.1$). These findings suggest negligible pre-existing heterogeneity in evacuation behaviors across different socioeconomic groups prior to the intervention, strengthening the validity of our causal analyses.

Examination of immediate intervention effects revealed substantial negative coefficients (I_0) across all SEGs in the control condition, indicating rapid evacuation behavior followingin response to the initial evacuation warning. The magnitude of this effect exhibited a positive correlation with socioeconomic status ($I_0^{Low} = -0.393$, $I_0^{Med} = -0.463$, $I_0^{High} = -0.675$), suggesting heightened reactivity to warning messages among higher SEGs. The group-intervention interaction term (GI_0) demonstrated additional negative effects that were inversely proportional to socioeconomic status ($GI_0^{Low} = -0.360$, $GI_0^{Med} = -0.242$, $GI_0^{High} = -0.114$). This pattern indicates that the evacuation mandate had a more pronounced impact on lower SEGs, suggesting these groups may be less inclined to evacuate without explicit governmental directives.

Post-intervention return patterns revealed positive trend changes (T_{I_0}) across all groups, with the majority of tower locations showing population recovery within 12 h of evacuation. The control group demonstrated a socioeconomic gradient in return rates, with higher SEGs exhibiting stronger coefficients ($T_{I_0}^{High} = 0.045$, $T_{I_0}^{Med} = 0.031$, $T_{I_0}^{Low} = 0.026$), corresponding to approximately

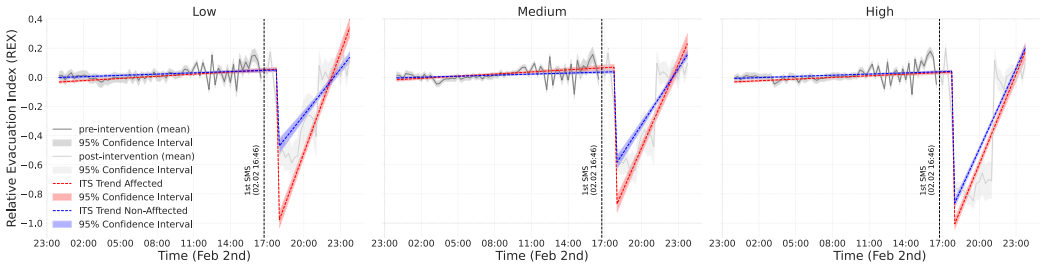

Fig. 6. Controlled Interrupted Time Series (CITS) stratified by three SEGs (Low (left), Medium (center), High (right) for February 2nd, 2024. We display the pre-intervention (dark-gray) and post-intervention (light-gray) observed REX. The red line (and red bands) represent the predicted REX trend (and 95% CI) for the affected group using CITS analysis. The blue line (and blue bands) represents the predicted REX trend (and 95% CI) for the control group using CITS analysis.

5% REX recovery per 15-minute interval in high SEG areas. The group-trend interaction terms (GT_{I_0}) exhibited additional positive effects that were inversely proportional to socioeconomic status ($GT_{I_0}^{Low} = 0.030$, with diminishing magnitudes as SEG increased), indicating accelerated population return rates among lower SEGs in affected communities. Note that a faster return rate does not necessarily mean a faster recovery to pre-intervention values, as the lower SEGs exhibit a stable but sustained pattern of hyperactivity during the entire day of Feb 3rd. Nevertheless, the CITS models for February 3rd show that the first warning message of the second day did not have the same mobilizing effect as in the previous day. In this case, we do not see a significant impact for not affected towers either immediately (I_0) or in the longer trend (T_{I_0}), thus suggesting that these communities had already overcome the initial rush of the event. Also, the observed impact for the affected towers is one order of magnitude smaller than the day before (see also Fig. E.13).

The quantitative evidence for alert fatigue is further supported by the noticeable reduction in model explanatory power between the two days. The CITS models for February 2nd demonstrate strong explanatory capacity with R-squared values ranging from 0.289 to 0.427 across socioeconomic groups, indicating that our model successfully captures systematic behavioral patterns followingin response to the initial alerts. In stark contrast, the February 3rd models show exceptionally low R-squared values (0.025-0.032), indicating that less than 3.2% of the variance in population movement can be explained by our systematic intervention model. This ten-fold reduction in explanatory power suggests that the predictable, systematic evacuation behaviors observed on the first day largely disappeared on the second day, providing quantitative evidence that subsequent alerts failed to generate coherent population responses comparable to the initial warning. These results support the hypothesis of a diminished effect/alert fatigue for subsequent rounds of messages during a critical event.

Our results revealed three main findings regarding socioeconomic disparities in evacuation behavior (Fig. 6). First, higher socioeconomic groups demonstrated heightened immediate responsiveness afterto warning messages, as evidenced by larger negative intervention coefficients (I_0). Second, lower socioeconomic groups exhibited stronger differential effects between treatment and control conditions, manifested in both immediate response (GI_0) (see Fig. E.15) and temporal trends (GT_{I_0}). Third, while higher socioeconomic groups showed more rapid recovery patterns (T_{I_0}), lower socioeconomic groups in affected areas demonstrated accelerated differential return rates (GT_{I_0}). These findings suggest complex socioeconomic heterogeneity in both evacuation decision-making and subsequent return behavior.

To formally assess SEG differences, we estimated the interrupted time series model using a pooled specification with socioeconomic group interactions (Low, Medium, High). Table E.4 (Supplementary Material) presents the full regression results. The pooled model confirms that post-intervention effects differ systematically by socioeconomic group. The observed pattern reinforces our earlier conclusions.

4. Discussion

Our near-real-time (one-day delay) connectivity analysis of the Valparaíso wildfires provides quantitative assessments addressing research questions on timing effects, socioeconomic disparities, and spatial consequences of emergency alerts. By integrating high-resolution data with a structured evaluation framework, we offer empirical validation of evacuation behavior and emergency communication effectiveness, extending prior research on disaster response.

Our first finding suggests potential alert fatigue. The initial evacuation alert triggered an immediate response, with connectivity dropping by over 80% in some areas within 1 h and 30 min, while subsequent alerts showed diminishing effects. Repeated exposure to frequent alerts may reduce responsiveness to actual threats, as previously observed during the Los Angeles wildfires [3,34]. Also, the dramatic drop in model explanatory power from 28.9–42.7% on February 2nd to just 2.5–3.2% on February 3rd provides quantitative evidence for alert fatigue, as systematic evacuation behaviors became largely unpredictable on the second day. These observations contribute to the existing literature by providing near-real-time quantitative assessments of evacuation warnings, as erosion of trust in emergency messaging can lead to delays in life-saving evacuations [33]. Integrating these insights into evacuation alert administration may minimize redundant messages while maintaining public confidence in emergency communication systems.

The second key finding highlights socioeconomic disparities in evacuation patterns [35,42]. Lower socioeconomic groups (SEGs) were more impacted by the evacuation alert, taking more time not only to evacuate but also to return to normality [5,8]. We observed that high-income SEGs evacuated and returned to normal activity faster, suggesting that populations in wealthier regions experience fewer barriers to evacuation and recovery, likely due to alternative housing options. Given these patterns, communication systems could integrate return-safety notifications to prevent premature re-entry into hazardous areas [5,43].

The third key finding concerns evacuation in non-warned areas. High-SEG populations showed less differentiation between warned and non-warned areas, indicating a tendency for precautionary evacuation even without official directives. In contrast, lower-income populations exhibited a stronger differential response between warned and non-warned areas, suggesting a greater reliance on government-issued alerts for evacuation decisions [4,8]. In non-warned areas, we measured connectivity reductions of −0.47 for low-SEG, −0.56 for medium-SEG, and −0.81 for high-SEG, indicating varied levels of evacuation based on perceived risk [5,6]. While voluntary evacuations can reduce fatalities, they can also increase transportation congestion and strain emergency response infrastructure [39].

The spatial diffusion of evacuation behavior beyond targeted areas presents challenges for geographic precision in alert dissemination and resource allocation, a concern previously noted in wildfire evacuation studies [44]. Our work contributes to the understanding of risk communication theory and digital crisis response mechanisms by quantifying voluntary evacuations as they occur.

Despite its strengths, this study has methodological limitations. Reliance on mobile phone data from a single carrier, which represents 28% of the market, may under-represent certain population segments [45]. Additionally, socioeconomic classification based on census data may obscure within-zone heterogeneity, limiting our analysis granularity. Attribution of behavioral changes solely to evacuation alerts presents another challenge, as evacuation decisions are influenced by multiple factors, including media coverage, social networks, and direct observation of fire conditions [6]. While our CITS methodology mitigates some concerns by comparing affected and non-affected areas, it cannot fully isolate the effect of evacuation alerts from other sources. Furthermore, our REX measure captures relative population movement (in the sense that if there is less activity in a given tower, this means that devices that were once there, are not anymore) but does not distinguish between permanent evacuation, temporary relocation, or routine mobility, potentially affecting the interpretation of post-alert movement patterns. Moreover, REX captures relative population egress rather than individual destinations. Negative REX values in warned and non-warned towers point to a broader regional redistribution of devices, with many evacuees plausibly relocating to adjacent municipalities or Santiago, as some anecdotal and local-media accounts suggest. We also recognize that connection counts do not translate directly into absolute population numbers, nor can decreases be interpreted as precise evacuation rates. Several factors (including temporary reductions in mobile use, short-term network congestion, or localized infrastructure damage)could contribute to drops in connectivity independent of physical movement. Our CITS design with non-warned towers as a baseline aims to mitigate these concerns. Furthermore, the interpretation of REX during recovery periods requires particular caution. While a return to baseline REX values might suggest population recovery, our metric cannot distinguish between the return of original residents and the presence of other groups, such as emergency responders, journalists, relief workers, or new occupants. This ambiguity limits our ability to make definitive claims about community resilience or true 'return to normal.'

However, several factors suggest this limitation likely should have minimal impact on our main findings. First, the scale difference between resident populations (tens of thousands) and temporary responders (typically hundreds) indicates that non-residents would constitute a relatively small fraction of observed connectivity. Second, emergency responders and media typically concentrate in specific high-impact zones rather than distributing uniformly across affected areas, which would produce distinct spatial patterns different from the broad recovery patterns we observe. Third, the gradual REX recovery over 8+ hours and sustained elevated activity (20% above baseline for low-SEG, 10% for medium-SEG) are more consistent with residents returning and resuming modified routines than with emergency personnel deployment patterns.

Nevertheless, without additional data sources to validate population composition, we cannot definitively rule out some contribution from non-resident populations. Future work incorporating emergency service deployment records or survey data could help disentangle these different populations and provide a more nuanced understanding of post-disaster recovery dynamics, particularly as different socioeconomic areas might attract varying levels of emergency response and media attention.

Future research should explore multi-channel emergency communication, comparing the effectiveness of evacuation alerts, social media updates, and emergency broadcast systems to determine optimal strategies for different socioeconomic groups [12,28]. Longitudinal studies tracking alert responsiveness across multiple disasters could identify desensitization patterns and develop countermeasures to maintain public engagement with warnings. Research should also examine how linguistic framing, information sequencing, and geographic specificity influence evacuation compliance [46]. Integrating near-behavioral data with survey methods could deepen our understanding of how individuals interpret and act upon emergency messages. Computational modeling using mobile network data could refine evacuation predictions and improve emergency response simulations, enabling authorities to optimize alert strategies before future crises [31].

Our findings reveal insights for disaster management that may help refine evacuation protocols to implement multi-tiered, phased evacuations. Prior research, primarily based on interviews and surveys, has evidenced similar patterns of socioeconomic evacuation inequalities, particularly regarding transportation access and trust in authorities [8]. We contribute to current literature by providing quantification of evacuation patterns as they occur, illuminating temporal and socioeconomic evacuation dynamics that complement survey-based approaches. These insights may help prioritize at-risk communities first, preventing bottlenecks and reducing transportation congestion [35]. Moreover, these refinements may enhance evacuation compliance, reduce infrastructure strain, and improve resource allocation during crises.

With climate change increasing wildfire severity, optimizing emergency communication systems is essential for population safety. The observed over-evacuation in non-targeted areas highlights the need for precision in alert dissemination to prevent infrastructure congestion [6]. Our findings support the benefits of integrating mobile connectivity patterns into disaster management, a critical adaptation pathway for societies facing increasing climate-driven hazards.

5. Methods

Data description and connectivity measure. We analyzed three primary data sources: (1) anonymized eXtended Detail Records (XDRs) from Telefónica Movistar, representing 28% market share in Chile as of June 2024 [45]; (2) emergency alert messages provided by SENAPRED (National Emergency Service); and (3) 2017 Census data from the National Institute of Statistics of Chile.

The mobile network data covered two comparison periods with identical day-of-week compositions: a baseline period (January 25–28, 2024, Thursday–Sunday) and the fire event period (February 1–4, 2024, Thursday–Sunday). This design controls for systematic weekday/weekend connectivity variations, allowing us to isolate the effects of wildfire alerts from routine temporal variations. The study area encompassed the Valparaíso region, covering approximately 23,015 square kilometers with 6977 cells mounted on 595 towers (Base Transceiver Stations) included in the analysis. The analysis included 587 towers during baseline and 588 towers during the fire period. Tower density averaged 7 cells per square kilometer in urban areas and .1 cells per square kilometer in rural zones (although rural cells are high-power antennas that serve large areas). Of all the cells analyzed, 33% (2294) were in rural areas and 67% (4683) were in urban areas. The data set contains the events of all the devices in the network. We have shown in other works that this is highly correlated with census information in terms of population distributions [37,38]. XDRs capture detailed metadata on mobile network activities, offering temporally granular insights into user behaviors.

XDR events were aggregated at 15-minute intervals, providing 2989 ± 524 temporal observations per tower across the study period. The baseline period contained 77,781,955 total records with a mean of 335 unique device IDs ($\sigma = 342$) per time interval. The fire period contained 83,335,714 records with a mean of 368 unique device IDs ($\sigma = 404$) per interval. This temporal granularity allowed detection of rapid behavioral changes following evacuation alerts. Activity patterns showed expected circadian variations, with peak connectivity during daylight hours (1,095,361 maximum connections at 17:30) and minimum activity during early morning (541,564 minimum connections at 05:00). This baseline served as a reference for normal tower usage patterns, enabling direct comparison with connectivity patterns observed during the wildfires. XDR tuples (n, t, A, k), were processed where n represents the anonymized device ID, t represents the timestamp, A represents the tower identifier, and k represents data volume in kilobytes [47]. Timestamps were rounded down to the nearest 15-minute block. Device counts were aggregated by tower and time interval to generate connectivity metrics (what we call “connectivity patterns”). Notice that there is one way in which this is akin to a simple mobility measure: IDs that are no longer present in one tower are supposed to have moved to another, unknown one. No individual trajectories were reconstructed, preserving privacy while enabling population-level analysis.

Unlike GPS-based mobility datasets (e.g., Cuebiq, SafeGraph), which rely on opt-in location-sharing from specific applications and typically capture only a subset of the population with inherent sampling biases toward smartphone users with particular apps installed, XDRs represent network-level events that capture all devices actively using the network regardless of device type, operating system, or user consent for location tracking. This comprehensive coverage eliminates self-selection bias and provides a more representative sample of the population, particularly including demographic groups less likely to use location-enabled applications. Furthermore, XDRs offer consistent temporal coverage as they record all network interactions rather than periodic location pings, enabling detection of rapid behavioral changes with higher reliability. While GPS data provides precise geographic coordinates, the tower-level granularity of XDRs proves sufficient for population-scale analyses while naturally preserving privacy through spatial aggregation, making them particularly suitable for emergency response research where population coverage and representativeness are paramount.

Identifying warned towers. The messages were provided to us in an Excel sheet in the following form: `date`, `hour`, `event`, `threat`, `message`, `polygon`, `region`, `X`. The `date` and `hour` fields were two separate fields in the format DD/MM/YYYY and HH:MM, respectively, the latter in the 24-hour format. The first message was time-stamped with `date 2/2/2024` and `time 16:45`. The `event` was of type `Evacuación (Incendio Forestal)` (tr. Evacuation (Forest Fire)). `threat` was `Incendio Forestal` (tr. Forest Fire). The `message` was `SENAPRED: Por incendio forestal evacue sector Quebrada Escobares, comuna de Villa Alemana` (tr. SENAPRED: Due to a forest fire, evacuate the Quebrada Escobares sector, Villa Alemana commune). `polygon` was `Comuna de Villa Alemana` (tr. Commune of Villa Alemana); `region` was the affected region, in the case of the first message, it was `Valparaíso` and finally `X` was the X/Twitter message sent. In the first message, this was https://twitter.com/Senapred/status/1753503622174761190. Unfortunately, the information did not include a “real" polygon of any affected areas, according to the evacuation alert. There was only a general area to which the language alluded. In the above message, this was Quebrada Escobares, east of the town of Quilpué. To formalize this and provide a more specific area, we took all the unique places mentioned in all alerts that were sent and used the Nominatim geocoding service[1] to retrieve the latitude and longitude coordinates for each place. These identified places are the green dots in Fig. 1B. The 5 km of the affected towers were identified as originating from these points. All towers that were not warned were used as controls; see the study design below.

[1] https://nominatim.org/

Assigning socio-economic groups. Due to the lack of reliable self-reported socioeconomic data, we estimated a tower's socioeconomic status based on its location. We used 2017 census data from the National Institute of Statistics of Chile to classify the location of the towers into three socioeconomic categories: Low, Middle, and High. To estimate socioeconomic status, we first assigned it to the entire census zone, using the proportion of individuals with higher education as an indicator. We also assessed the correlation between educational level and the Socio-Material Territorial Index,[2] which yielded a high correlation coefficient of $\rho = 0.93$ [48]. We decided to use only educational level, as the methodology behind the Socio-Material Territorial Index is less interpretable. Once we had the socioeconomic index, we divided census zones into socioeconomic categories using population quantiles. This ensured a balanced representation across groups and maintained adequate sample sizes for each category. After determining the socioeconomic status for all census zones, we assigned these zones' status to the communication towers located within them. Each census zone, on average, contains 1.53 telecommunication towers and has a total population of approximately 2436 individuals. This classification approach allowed us to identify key behavioral trends and differences between socioeconomic groups while maintaining a balance and avoiding overly detailed subdivisions that might obscure meaningful patterns.

Calculating relative evacuation. As introduced in Section 3.3, the Relative Evacuation Index (REX) represents the proportional reduction (increase) in mobile device connections relative to baseline patterns. It is calculated as $\text{REX}=(n_t - n_b)/n_t + n_b$, where, for a given tower, n_t represents the number of unique mobile devices detected at time t, and n_b denotes the device count for the corresponding tower for the same day-of-week and same time-of-day during baseline days. This formulation produces values ranging from -1.0 (indicating a complete population egress — with no connections at time t) to positive values (indicating population ingress for this tower).

For our temporal dynamics analyzes, we also show results using a simpler evacuation rate in percentage (i.e., $(n_t/n_b) * 100$). This percentage offers more straightforward interpretability for the aggregated cumulative distribution. For example, an evacuation rate of -75% indicates that tower connections dropped to 25% of baseline levels, while a rate of -50% means connections fell to half the baseline count.

Note that, in any case, our study does not claim a one-to-one mapping between device connections and the absolute number of people in the area. Instead, we interpret sudden, spatially structured deviations from carefully matched baseline patterns as a relative indicator of collective movement. Thus, we use REX to measure near-real-time displacement intensity and timing rather than a literal count of evacuees or their ultimate locations.

Study design and statistical analysis. We employed a quasi-experimental design using a controlled interrupted time series (CITS) to assess behavioral responses followingto wildfire warning messages [49,50]. For this study, we defined the control group based on geolocation data, selecting cellular towers that were never directly addressed by the warning SMSs and, therefore, should have remained unaffected by the wildfires. Although individuals connected to these non-warned towers may have been exposed to warning messages, their behavioral response is expected to be primarily preventive. To account for response latency, we incorporated a delayed intervention effect, informed by previous studies on emergency evacuations, which indicate reaction delays due to factors such as health status, social influences, and affiliations [51,52]. Model calibration across a range of delays identified 1 h and 15 min as the optimal lag for capturing observed evacuation patterns (Supplementary Fig. E.12). We estimated the intervention effect using the following CITS model:

$$Y = \beta_0 + \beta_1 T + \beta_2 I_0 + \beta_3 T_{I_0} + \beta_4 G + \beta_5 GT + \beta_6 G I_0 + \beta_7 G T_{I_0} + \epsilon \tag{1}$$

where Y represents the predicted REX, T denotes time (measured in 15-minute intervals), I_0 is a post-event indicator set to 1 after the intervention (incorporating the delay), and T_{I_0} captures the trend change following the intervention. G distinguishes between the affected and control groups. The Newey–West variance estimator was used to correct for heteroskedasticity and autocorrelation, ensuring robust inference. For completeness, we also include in the Supplementary Materials the results from the uncontrolled Interrupted Time Series analysis for the entire observed period (Table E.3 and Fig. E.14).

Abbreviations

- **BIC** - Bayesian Information Criterion
- **CDR** - Call Detail Records
- **CI** - Confidence Interval
- **CITS** - Controlled Interrupted Time Series
- **CLST** - Chile Standard Time
- **FCC** - Federal Communications Commission
- **ITS** - Interrupted Time Series
- **ITU** - International Telecommunication Union
- **REX** - Relative Evacuation Index
- **SAE** - Sistema de Alerta de Emergencia (Emergency Alert System in Chile)
- **SEG** - Socio-Economic Group
- **SMS** - Short Message Service
- **WEA** - Wireless Emergency Alerts
- **XDR** - eXtended Detail Records

[2] More detailed information about this index is available at: thislink (in Spanish).

Table A.2
Time of the SMSs that included new affected towers in the warning message. The data shows the number of new towers warned by each SMS stratified by socio-economic groups.

ID	Datetime	High	Medium	Low
0	2024-02-02 16:45	2	0	0
1	2024-02-02 18:30	12	12	4
2	2024-02-02 18:45	4	8	3
3	2024-02-02 19:45	0	7	6
4	2024-02-02 21:15	1	1	0
5	2024-02-03 10:45	1	0	1
6	2024-02-03 12:15	4	1	3
7	2024-02-03 13:00	1	2	0
8	2024-02-03 14:15	6	6	2
9	2024-02-03 14:30	0	1	1
10	2024-02-03 15:00	17	0	0
11	2024-02-03 17:00	0	1	0
12	2024-02-03 18:00	2	0	6
13	2024-02-03 18:30	0	0	2
		50	**39**	**27**

CRediT authorship contribution statement

Erick Elejalde: Writing – review & editing, Writing – original draft, Visualization, Validation, Methodology, Investigation, Formal analysis, Data curation, Conceptualization. **Timur Naushirvanov:** Writing – review & editing, Methodology, Investigation, Conceptualization. **Kyriaki Kalimeri:** Writing – review & editing, Writing – original draft, Methodology, Formal analysis, Conceptualization. **Elisa Omodei:** Writing – review & editing, Supervision, Methodology, Conceptualization. **Márton Karsai:** Writing – review & editing, Supervision, Methodology, Funding acquisition, Formal analysis, Conceptualization. **Loreto Bravo:** Writing – review & editing, Resources, Methodology, Conceptualization. **Leo Ferres:** Writing – review & editing, Writing – original draft, Resources, Project administration, Methodology, Funding acquisition, Formal analysis, Data curation, Conceptualization.

Declaration of competing interest

The authors declare the following financial interests/personal relationships which may be considered as potential competing interests: Leo Ferres reports financial support was provided by National Fund For Scientific Technological and Technological Innovation Development. Leo Ferres reports financial support was provided by CRT Foundation. Marton Karsai reports financial support was provided by National Laboratory for Health Security. Marton Karsai reports financial support was provided by French National Research Agency. Marton Karsai reports financial support was provided by Horizon 2020 European Innovation Council Fast Track to Innovation. If there are other authors, they declare that they have no known competing financial interests or personal relationships that could have appeared to influence the work reported in this paper.

Appendix A. List of considered warning SMSs

See Table A.2.

Appendix B. Average number of unique devices per antenna by socioeconomic group

See Fig. B.7.

Appendix C. Cumulative distribution functions considering tower-level REX

See Figs. C.8 and C.9.

Appendix D. Rex timeline for affected towers segregated by the time of their first notification

See Figs. D.10 and D.11.

Appendix E. Time series analysis

See Figs. E.12 and E.15.

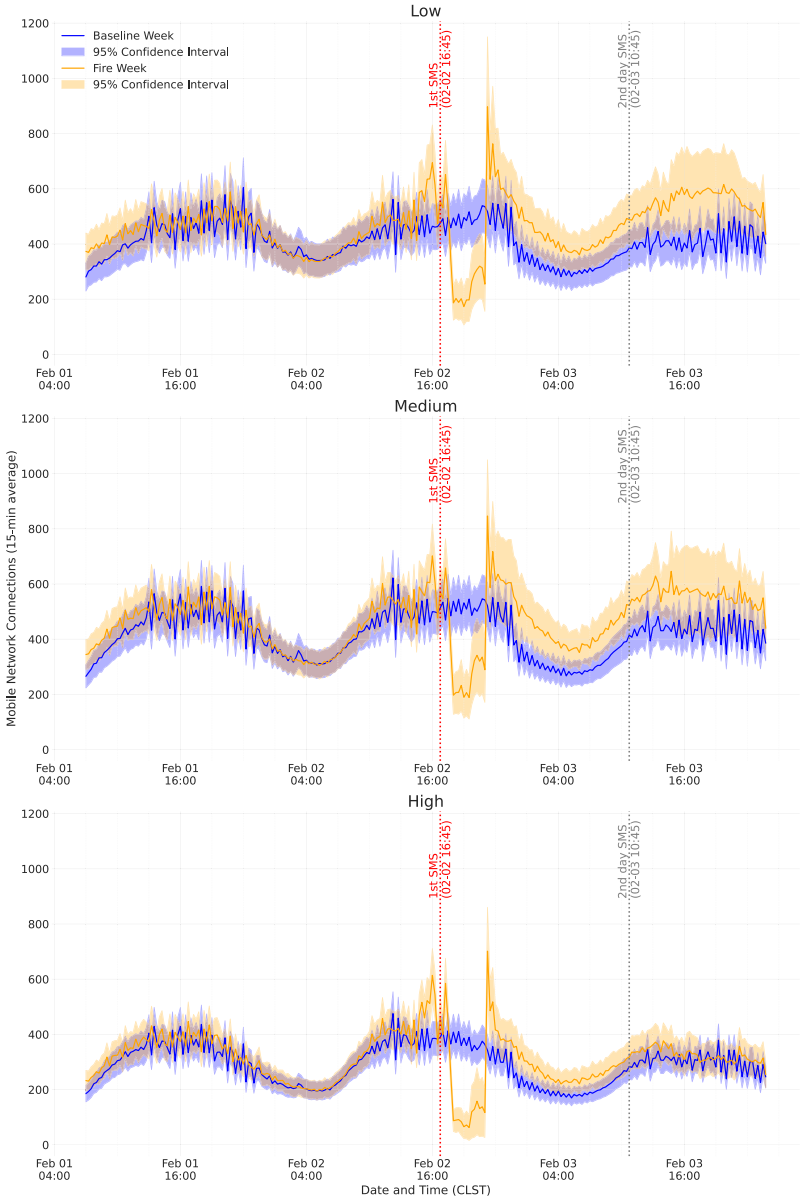

Fig. B.7. Mobile phone tower connectivity patterns during a wildfire evacuation event by socio-economic group: low (top), medium (middle) and high (bottom).

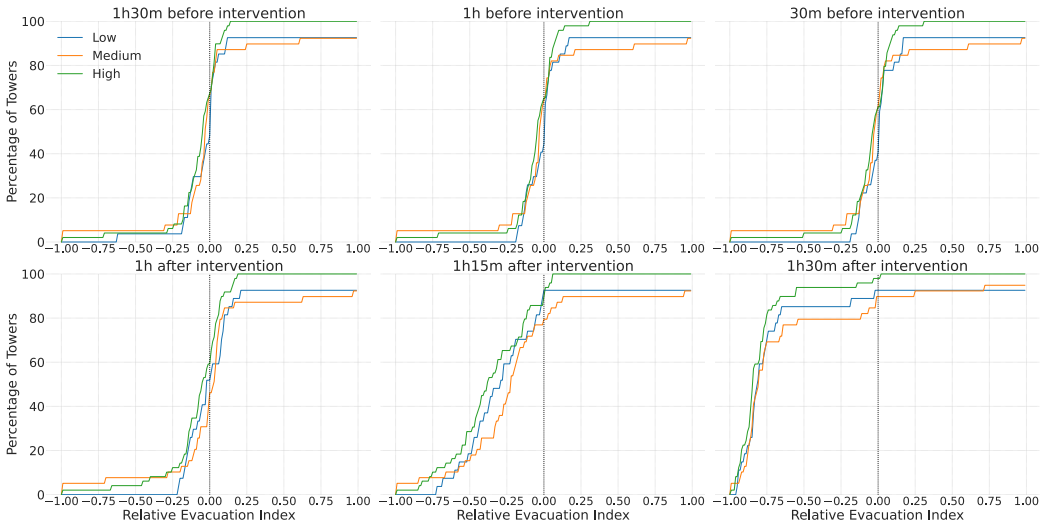

Fig. C.8. Cumulative distribution functions (CDFs) of tower-level REX, stratified by socioeconomic status. The figure presents six time-sliced CDFs capturing population displacement patterns before and after the intervention across low (blue), medium (orange), and high (green) socioeconomic areas. Pre-intervention panels show behavior at 1.5 h, 1 h, and 0.5 h (30 min), while post-intervention panels display changes at 1 h, 1 h and 15 min, and 1 h and 30 min. The *x*-axis represents the observed REX, where 0 indicates behavior consistent with the baseline days, negative values indicate evacuation relative to baseline, and positive values represent more connections relative to baseline. The *y*-axis shows the cumulative percentage of towers exhibiting REX lower than or equal to the corresponding x-value up to this time.

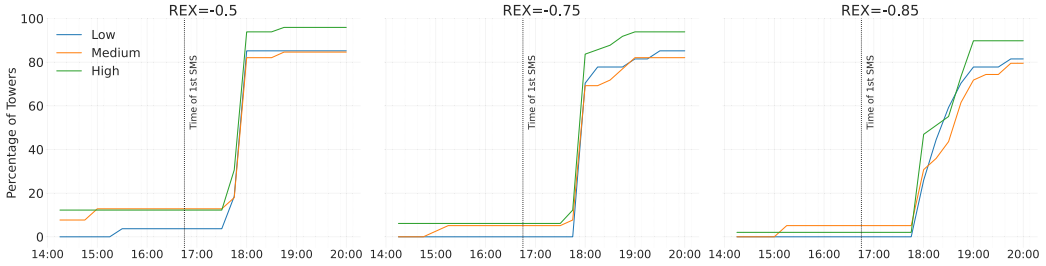

Fig. C.9. Cumulative distribution function of tower REX over time. The *x*-axis represents time, while the *y*-axis indicates the percentage of towers that reached the specified REX rates (−0.50, −0.75, and −0.85). The lines are stratified by socio-economic groups (SEGs): low (blue), medium (orange), and high (green). The dashed line marks the time at which the first evacuation SMS was sent.

Table E.3
Interrupted Time Series (ITS) Analysis (uncontrolled) for different Socio-Economic Groups (SEG).

	Socio-Economic Groups		
	Low	Medium	High
Intercept	−0.02***	0.043***	0.039***
	(−0.027–0.012)	(0.036-0.05)	(0.033-0.045)
T	0.001***	0.0	0.0***
	(0.001-0.001)	(0.0-0.0)	(−0.001–0.0)
I_0	−0.786***	−0.666***	−0.724***
	(−0.829–0.742)	(−0.71–0.623)	(−0.755–0.694)
T_{I_0}	0.057***	0.048***	0.052***
	(0.052-0.061)	(0.043-0.052)	(0.048-0.055)

Note: $^{**}p < 0.01$; $^{***}p < 0.001$

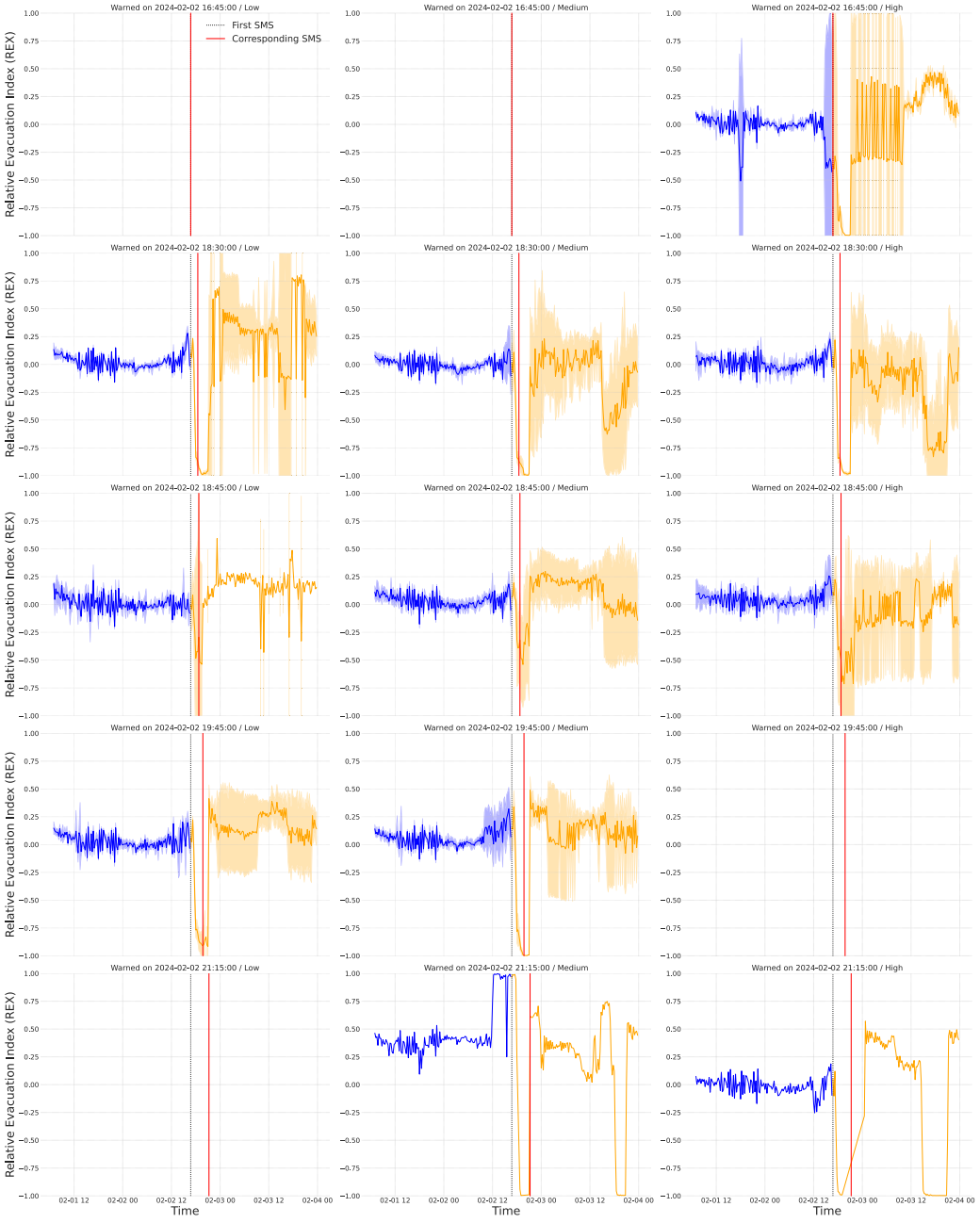

Fig. D.10. REX for affected towers notified on the first day of the wildfires. Every row represents the evacuation behavior for affected towers that were notified for the first time in the corresponding warning SMS. Columns represent different Socio-Economic Groups (SEG).

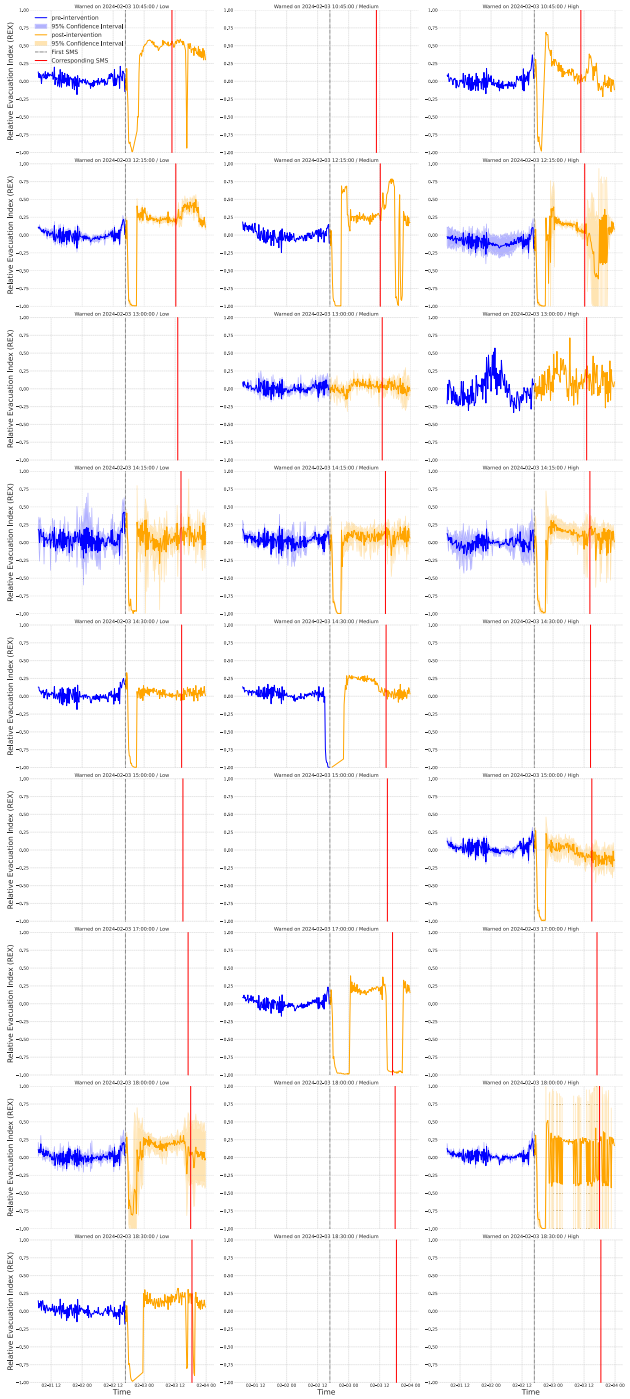

Fig. D.11. REX for affected towers notified on the second day of the wildfires. Every row represents the evacuation behavior for affected towers that were notified for the first time in the corresponding warning SMS. Columns represent different Socio-Economic Groups (SEG).

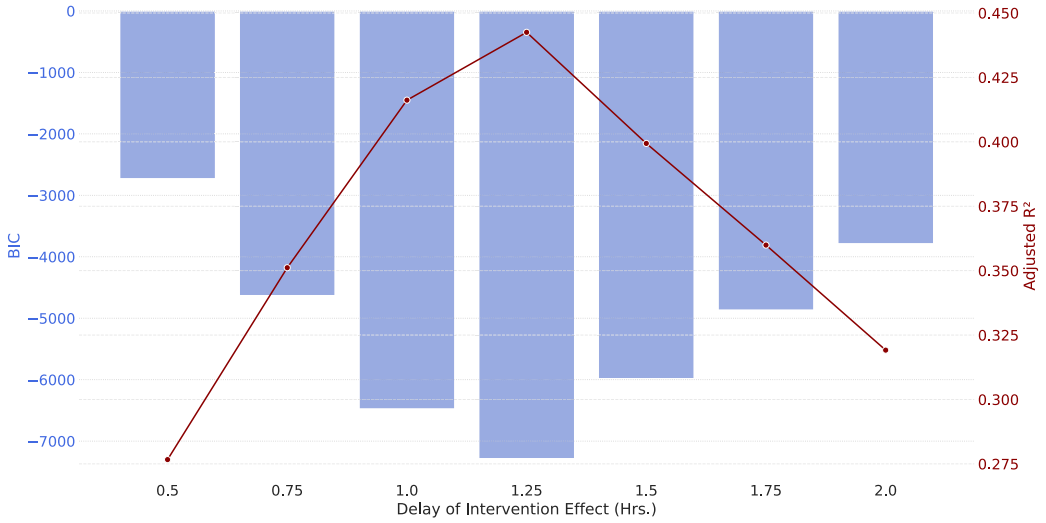

Fig. E.12. Comparison between Interrupted Time Series (ITS) models for affected towers with different delays. The x-axis represents the range of delays tested in 15-minute steps (from 30 min (0.5 Hrs.) to 120 min (2.0 Hrs.)). The bars represent the BIC for the regression using the corresponding delay (left y-axis). The line plot represents the Adjusted R^2 for the regression using the corresponding delay (right y-axis).

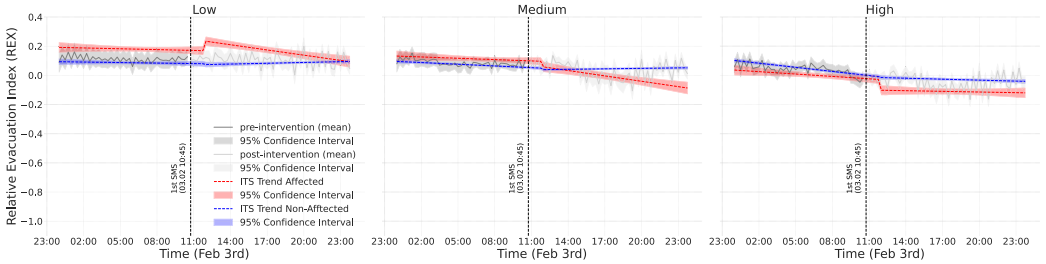

Fig. E.13. Controlled Interrupted Time Series (CITS) stratified by three socio-economic groups (Low (left), Medium (center), High (right) for February 3rd. The data displays the pre-intervention (dark-gray) and post-intervention (light-gray) observed REX. The red line (and red bands) represent the predicted REX trend (and 95% CI) for the affected group using CITS analysis. The blue line (and blue bands) represent the predicted REX trend (and 95% CI) for the control group using CITS analysis.

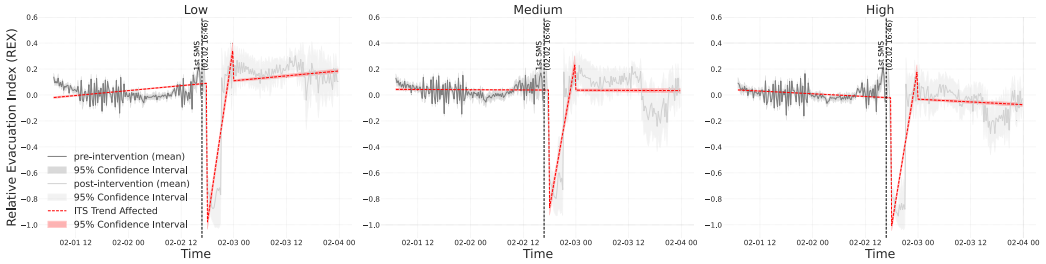

Fig. E.14. (Uncontrolled) Interrupted Time Series (ITS) stratified by three socio-economic groups (Low (left), Medium (center), High (right) from February 1-3. The data displays the pre-intervention (dark-gray) and post-intervention (light-gray) observed REX. The red line (and red bands) represent the predicted REX trend (and 95% CI) for the affected group using ITS analysis.

Table E.4
Pooled controlled interrupted time-series regression with socioeconomic group interactions. Dependent variable: normalized tower connectivity (REX).

	Coefficient	Std. Error	*p*-value
Main effects			
I_0 (overall)	−0.383	0.007	<0.001
T_{I_0} (post slope change)	0.026	0.001	<0.001
G (affected tower)	−0.040	0.009	<0.001
Socioeconomic group effects			
SEG_{Low}	−0.014	0.012	0.247
$SEG_{Low} \times G$	−0.024	0.018	0.171
$SEG_{Low} \times I_0$	−0.010	0.016	0.537
$SEG_{Low} \times G \times I_0$	−0.181	0.025	<0.001
$SEG_{Low} \times T_{I_0}$	0.000	0.001	0.950
$SEG_{Low} \times G \times T_{I_0}$	0.018	0.002	<0.001
SEG_{Medium}	−0.007	0.010	0.446
$SEG_{Medium} \times G$	−0.014	0.018	0.451
$SEG_{Medium} \times I_0$	−0.080	0.015	<0.001
$SEG_{Medium} \times G \times I_0$	−0.063	0.025	0.011
$SEG_{Medium} \times T_{I_0}$	0.006	0.001	<0.001
$SEG_{Medium} \times G \times T_{I_0}$	0.003	0.002	0.257
SEG_{High}	−0.016	0.009	0.085
$SEG_{High} \times G$	−0.002	0.016	0.895
$SEG_{High} \times I_0$	−0.293	0.012	<0.001
$SEG_{High} \times G \times I_0$	0.065	0.019	0.001
$SEG_{High} \times T_{I_0}$	0.020	0.001	<0.001
$SEG_{High} \times G \times T_{I_0}$	−0.008	0.002	<0.001
Observations	34,136		
R-squared	0.369		

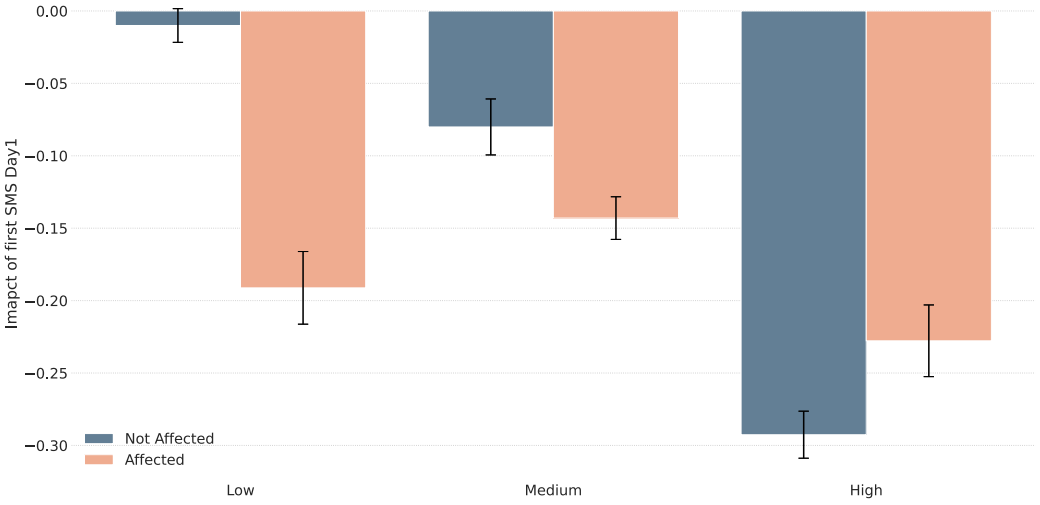

Fig. E.15. Estimated impact of the first SMS with pooled controlled interrupted time-series regression with socioeconomic group interactions.

Data availability

The data that has been used is confidential.

References

[1] M.W. Jones, D.I. Kelley, C.A. Burton, F. Di Giuseppe, M.L.F. Barbosa, E. Brambleby, A.J. Hartley, A. Lombardi, G. Mataveli, J.R. McNorton, F.R. Spuler, J.B. Wessel, J.T. Abatzoglou, L.O. Anderson, N. Andela, S. Archibald, D. Armenteras, E. Burke, R. Carmenta, E. Chuvieco, H. Clarke, S.H. Doerr, P.M. Fernandes, L. Giglio, D.S. Hamilton, S. Hantson, S. Harris, P. Jain, C.A. Kolden, T. Kurvits, S. Lampe, S. Meier, S. New, M. Parrington, M.M.G. Perron, Y. Qu, N.S. Ribeiro, B.H. Saharjo, J. San-Miguel-Ayanz, J.K. Shuman, V. Tanpipat, G.R. van der Werf, S. Veraverbeke, G. Xanthopoulos, State of wildfires 2023–2024, Earth Syst. Sci. Data 16 (8) (2024) 3601–3685, http://dx.doi.org/10.5194/essd-16-3601-2024.

[2] Y. Guo, J. Wang, Y. Ge, C. Zhou, Global expansion of wildland-urban interface intensifies human exposure to wildfire risk in the 21st century, Sci. Adv. 10 (45) (2024) eado9587.
[3] T. Guardian, Los angeles to review wildfire alert systems after lethal blazes, 2025.
[4] M. Cursino, Chile forest fires: More than 100 dead in valparaíso region, 2024, BBC News.
[5] M. Burke, S. Heft-Neal, J. Li, A. Driscoll, P. Baylis, M. Stigler, J.A. Weill, J.A. Burney, J. Wen, M.L. Childs, C.F. Gould, Exposures and behavioural responses to wildfire smoke, Nat. Hum. Behav. 6 (10) (2022) 1351–1361, http://dx.doi.org/10.1038/s41562-022-01396-6.
[6] K. McConnell, E. Fussell, J. DeWaard, S. Whitaker, K.J. Curtis, L. St. Denis, J. Balch, K. Price, Rare and highly destructive wildfires drive human migration in the us, Nat. Commun. 15 (1) (2024) 6631.
[7] Z. Wang, Z. Wang, Z. Zou, X. Chen, H. Wu, W. Wang, H. Su, F. Li, W. Xu, Z. Liu, J. Zhu, Severe global environmental issues caused by Canada's record-breaking wildfires in 2023, Adv. Atmospheric Sci. 41 (4) (2024) 565–571, http://dx.doi.org/10.1007/s00376-023-3241-0.
[8] R.R. Thompson, D.R. Garfin, R.C. Silver, Evacuation from natural disasters: a systematic review of the literature, Risk Anal. 37 (4) (2017) 812–839, Wiley.
[9] E. Ismagilova, L. Hughes, Y.K. Dwivedi, K.R. Raman, Smart cities: Advances in research—an information systems perspective, Int. J. Inf. Manage. 47 (2019) 88–100.
[10] International Telecommunication Union (ITU), Measuring Digital Development: Facts and Figures 2024, Tech. rep., International Telecommunication Union (ITU), 2024, copyright ©ITU 2024. All rights reservedURL https://www.itu.int/itu-d/reports/statistics/facts-figures-2024/.
[11] Subsecretaría de Telecomunicaciones de Chile (Subtel), Abonados móviles en chile - junio 2024, 2024, Subtel - Gobierno de Chile URL https://www.subtel.gob.cl/wp-content/uploads/2024/08/1_ABONADOS_MOVILES_JUN24_220824.xlsx. (Accessed 11 March 2025).
[12] Federal Communications Commission, Wireless Emergency Alerts (WEA), Tech. rep., Washington, DC, USA, URL https://www.fcc.gov/consumers/guides/wireless-emergency-alerts-wea.
[13] Cybersecurity, I. S. A. (CISA), Wireless emergency alerts (wea) general information, 2024, URL https://www.cisa.gov/sites/default/files/publications/Wireless%2BEmergency%2BAlerts%2B%28WEA%29%2BGeneral_0.pdf.
[14] G. Haddow, K.S. Haddow, Disaster Communications in a Changing Media World, Butterworth-Heinemann, 2013.
[15] Columbia University, The first sms emergency alert in sri lanka (2007), 2007, https://www.columbia.edu/itc/sipa/nelson/newmediadev/Emergencies.html.
[16] D. Coyle, P. Meier, New Technologies in Emergencies and Conflicts: The Role of Information and Social Networks, Tech. Rep., 2009.
[17] L.O. Danquah, N. Hasham, M. MacFarlane, F.E. Conteh, F. Momoh, A.A. Tedesco, A. Jambai, D.A. Ross, H.A. Weiss, Use of a mobile application for Ebola contact tracing and monitoring in northern Sierra Leone: a proof-of-concept study, BMC Infect. Dis. 19 (1) (2019) 810, http://dx.doi.org/10.1186/s12879-019-4354-z.
[18] A. Berman, M.E. Figueroa, J.D. Storey, Use of SMS-based surveys in the rapid response to the Ebola outbreak in Liberia: opening community dialogue, J. Health Commun. 22 (2017) 15–23, http://dx.doi.org/10.1080/10810730.2016.1224279.
[19] M.-A. Trad, R. Jurdak, R. Rana, Guiding Ebola patients to suitable health facilities: an SMS-based approach, F1000Research 4 (2015) 43, http://dx.doi.org/10.12688/f1000research.6105.1.
[20] M.M. Turner, S. Lisse, R. Rimal, T. Kamlem, H. Shaikh, N. Biswas, Rumour spread and control during the West African Ebola epidemic in Liberia, Disasters 47 (2) (2023) 346–365, http://dx.doi.org/10.1111/disa.12552.
[21] Wikipedia contributors, J-alert, wikipedia, the free encyclopedia, 2025, URL https://en.wikipedia.org/wiki/J-Alert. (Accessed 11 March 2025).
[22] J. Cinnamon, S.K. Jones, W.N. Adger, Evidence and future potential of mobile phone data for disease disaster management, Geoforum 75 (2016) 253–264, http://dx.doi.org/10.1016/j.geoforum.2016.07.019.
[23] E.J. Carlson, H. Bean, C. Ratcliff, M. Pokharel, J. Barbour, Do 360-character wireless emergency alert messages work better than 90-character messages? testing the risk communication consensus, J. Contingencies Crisis Manag. 32 (2) (2024) e12587.
[24] S. Gao, Y. Wang, Q. Wang, Household-targeted hurricane warnings for effective evacuation: Case study of hurricane irma in north miami beach, Constr. Res. Congr. 2022 (2022) 1116–1124.
[25] P. Slovic, Perception of risk, Science 236 (4799) (1987) 280–285.
[26] S.W. Durage, L. Kattan, S. Wirasinghe, J.Y. Ruwanpura, Evacuation behaviour of households and drivers during a tornado: Analysis based on a stated preference survey in calgary, Canada, Nat. Hazards 71 (2014) 1495–1517.
[27] E. Kuligowski, Evacuation decision-making and behavior in wildfires: Past research, current challenges and a future research agenda, Fire Saf. J. 120 (2021) 103129.
[28] S. N. E. O. of Chile, Sistema de alerta de emergencia (sae), 2024, URL https://cooperativa.cl/noticias/pais/desastres-naturales/mensajeria-sae-que-hacer-si-recibes-una-alerta-en-tu-celular/2023-06-24/153407.html.
[29] N. Dash, H. Gladwin, Evacuation decision making and behavioral responses: Individual and household, Nat. Hazards Rev. 8 (3) (2007) 69–77.
[30] R.C. Bonfanti, B. Oberti, E. Ravazzoli, A. Rinaldi, S. Ruggieri, A. Schimmenti, The role of trust in disaster risk reduction: a critical review, Int. J. Environ. Res. Public Health 21 (1) (2023) 29.
[31] T. Yabe, N.K. Jones, P.S.C. Rao, M.C. Gonzalez, S.V. Ukkusuri, Mobile phone location data for disasters: A review from natural hazards and epidemics, Comput. Environ. Urban Syst. 94 (2022) 101777.
[32] C. Calderara, Unión Europea hará una investigación externa para saber si el sistema de alerta SAE funcionó durante los incendios, 2024, p. T13, URL https://www.t13.cl/noticia/nacional/union-europea-hara-una-investigacion-externa-para-saber-si-sistema-alerta-sae-6-2-2024.
[33] D.S. Mileti, J.H. Sorensen, Communication of Emergency Public Warning: A Social Science Perspective, Westview Press, Boulder, CO, 1990.
[34] Associated Press, Too little, too late: Residents say they were in the dark as fire spread with no evacuation order, 2025, URL https://apnews.com/article/d78c30c9f73570c31aae9c9154c685ae.
[35] T. Yabe, K. Tsubouchi, N. Fujiwara, Y. Sekimoto, S.V. Ukkusuri, Understanding post-disaster population recovery patterns, J. R. Soc. Interface 17 (163) (2020) 20190532, http://dx.doi.org/10.1098/rsif.2019.0532.
[36] H. Deng, D.P. Aldrich, M.M. Danziger, J. Gao, N.E. Phillips, S.P. Cornelius, Q.R. Wang, High-resolution human mobility data reveal race and wealth disparities in disaster evacuation patterns, Humanit. Soc. Sci. Commun. 8 (1) (2021) 1–8.
[37] L. Gauvin, M. Tizzoni, S. Piaggesi, A. Young, N. Adler, S. Verhulst, L. Ferres, C. Cattuto, Gender gaps in urban mobility, Humanit. Soc. Sci. Commun. 7 (1) (2020) 11, http://dx.doi.org/10.1057/s41599-020-0500-x, publisher: Springer Science and Business Media {LLC}.
[38] E. Elejalde, L. Ferres, V. Navarro, L. Bravo, E. Zagheni, The social stratification of internal migration and daily mobility during the COVID-19 pandemic, Sci. Rep. 14 (1) (2024) 12140, http://dx.doi.org/10.1038/s41598-024-63098-5.
[39] S. Park, T. Yabe, S.V. Ukkusuri, Post-disaster recovery policy assessment of urban socio-physical systems, Comput. Environ. Urban Syst. 114 (2024) 102184, http://dx.doi.org/10.1016/j.compenvurbsys.2024.102184.
[40] X. Li, Y. Qiang, G. Cervone, Using human mobility data to detect evacuation patterns in hurricane ian, Ann. GIS 30 (4) (2024) 493–511.
[41] S. Hazarie, H. Barbosa, A. Frank, R. Menezes, G. Ghoshal, Uncovering the differences and similarities between physical and virtual mobility, J. R. Soc. Interface 17 (168) (2020) 20200250.
[42] Takahiro Yabe, T. Yabe, S.V. Ukkusuri, Effects of income inequality on evacuation, reentry and segregation after disasters, Transp. Res. Part D-Transport Environ. 82 (2020) 102260, http://dx.doi.org/10.1016/j.trd.2020.102260.
[43] T. Yabe, B.G.B. Bueno, M. Frank, A. Pentland, E. Moro, Behavior-based dependency networks between places shape urban economic resilience, 2023, http://arxiv.org/abs/2311.18108.

[44] X. Wang, G. Lindsey, S. Hankey, K. Hoff, Estimating mixed-mode urban trail traffic using negative binomial regression models, in: American Society of Civil Engineers, vol. 140, 2014, http://dx.doi.org/10.1061/(asce)up.1943-5444.0000157.
[45] Telefónica, Consolidated Annual Report 2023, Tech. rep., Madrid, 2024, URL https://www.telefonica.com/en/shareholders-investors/financial-reports/annual-report/.
[46] Y. Mejova, K. Kalimeri, Effect of values and technology use on exercise: Implications for personalized behavior change interventions, in: Proceedings of the 27th ACM Conference on User Modeling, Adaptation and Personalization, 2019, pp. 36–45.
[47] L. Pappalardo, L. Ferres, M. Sacasa, C. Cattuto, L. Bravo, Evaluation of home detection algorithms on mobile phone data using individual-level ground trut, EPJ Data Sci. 10 (1) (2021) http://dx.doi.org/10.1140/epjds/s13688-021-00284-9.
[48] T. Naushirvanov, E. Elejalde, K. Kalimeri, E. Omodei, M. Karsai, L. Ferres, Evacuation patterns and socioeconomic stratification in the context of wildfires in Chile, EPJ Data Sci. 14 (2025) 23, http://dx.doi.org/10.1140/epjds/s13688-025-00540-2.
[49] D. McDowall D. McDowall (Ed.), Interrupted time series analysis, nachdr, in: Edition, No. 21 in Quantitative Applications in the Social Sciences, Sage Publ, Newbury Park, Calif, 2003.
[50] J. Lopez Bernal, S. Cummins, A. Gasparrini, The use of controls in interrupted time series studies of public health interventions, Int. J. Epidemiol. 47 (6) (2018) 2082–2093, http://dx.doi.org/10.1093/ije/dyy135.
[51] R.F. Fahy, G. Proulx, et al., Toward creating a database on delay times to start evacuation and walking speeds for use in evacuation modeling, in: 2nd International Symposium on Human Behaviour in Fire, Boston, MA, USA, 2001, pp. 175–183.
[52] Y. Liu, Z. Zhang, Z. Mao, Analysis of influencing factors in preevacuation time using interpretive structural modeling, Saf. Sci. 128 (2020) 104785, http://dx.doi.org/10.1016/j.ssci.2020.104785.